

Optimizing Wheel Fairings for Fixed Gear Aircraft

Paul Holschneider¹, Addison Fisher¹ and Anat Fernandes[#]

¹The Buckley School, Sherman Oaks, USA

[#]Advisor

ABSTRACT

Fixed landing gear on aircraft inevitably increases drag and lowers aerodynamic efficiency. The use of wheel fairings in general aviation decreases drag, however, few studies have examined the optimization of fairing design. The current study begins to address the question of the aerodynamic effects of different designs of the wheel fairing's trailing edge. Wheel fairing models were created using Solidworks 2021 and 3d printed. The height of the trailing edge (percent of maximum fairing height, % height) was altered based on modern widely used fairing designs. Models were tested in a water channel and a small-scale wind tunnel. Force sensing and particle image velocimetry (PIV) were conducted to determine an improved design of the fairing's trailing edge and the resulting aerodynamic effects. Time averaged chordwise flow separation and the resulting velocity deficit were analyzed along with the drag force. Housing the wheel inside a fairing dramatically decreased vorticity (a measure of rotation in a fluid), increased the wake velocity, while decreasing the drag force. Compared to a 30% height fairing, the 0% height fairing (pointed trailing edge) created a broader area of elevated vorticity and velocity deficits in its wake in the water channel. It also resulted in a larger drag force as assessed in the wind tunnel. This study highlights that altering design of the trailing edge by increasing its height from 0% height to a broader profile can improve efficiency of fairings.

Introduction

Landing gear, while an essential component for most modern aircraft, inevitably increases parasitic drag, decreasing aircraft performance (Götten, 2018). To reduce this drag, most fixed gear aircraft in general aviation implement wheel fairings (Figure 1) to streamline the complex landing gear structure, often housing hydraulics, brake pads, oleo struts, etc. While general aviation aircraft often use wheel fairings, typically no two designs look alike, with frequent alterations in the height of the trailing edge of the fairing. There is a lack of published research focused on optimizing the aerodynamic parameters of fairing designs, with much of the research of private companies remaining outside the public realm.

The use of wheel fairings to minimize drag (Figure 2) has been reported in a few studies. Many of these focus, however, on either the presence or lack of gear fairings, not which gear fairing type is optimal. A few studies do suggest that fairings should be shaped to be rounded in the front and should gradually taper towards the trailing end. Some published studies have typically employed the use of two-dimensional models and simple geometric shapes for their testing. Ablog et al. used a circular disk to represent the wheel and simple geometric shapes to vary the fairing type (Ablog et al., 2014). Although these 2-D models can give us an idea of the most aerodynamic side profile for wheel fairings, this testing does not address the drag of the entire fairing.

There has been minimal research on the optimal shape of its trailing end. The trailing end of many wheel fairings is elliptically shaped, while others are shaped with more advanced geometric designs. The current exploratory study begins to address the question of the aerodynamic effects of different heights of the wheel fairing's trailing edge. Models were tested in a water channel and a small-scale wind tunnel. Force sensing and particle image velocimetry (PIV) were conducted to determine an improved design of the fairing's trailing edge and the resulting aerodynamic effects. Optimizing fairing design according to the aerodynamic effects could

result in increased efficiency (Herrnstein and Biermann, 1934; Wojnar, 1967), reduced carbon emissions, lowered operating costs, and noise reduction.



Figure 1. Example of a wheel fairing of a Cessna 150 (Ablog et al., 2014)

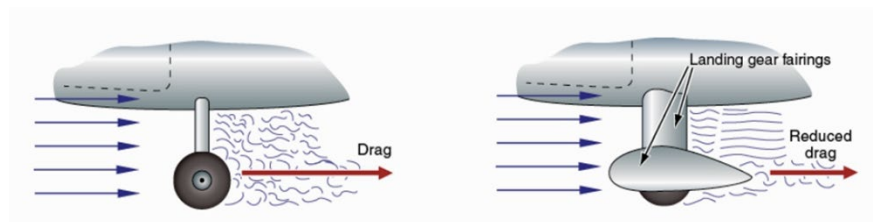


Figure 2. A representation of airflow over landing gear with and without fairings. Increased turbulence is seen in the wheel without fairings (left) (Aviation Supplies Academics, 2016).

Methods

List of Symbols

- c Chord length
- Re Reynolds number ($Re = \rho uL/\mu$)
- U_∞ Free stream velocity
- α Angle of attack
- u Local horizontal velocity
- Fd Drag force
- ρ Density of the fluid
- μ Dynamic viscosity of the fluid
- L Characteristic linear dimension

Fairing Design

All models tested were created using SOLIDWORKS (Dassault Systèmes, USA, version 2021). For experimentation, the height of the trailing edge was measured as a percentage of the maximum height of the fairing. Models were tested with a 0% height (0%H, i.e. pointed trailing edge), 15% height (15%H), and 30% height (30%H), where % refers to the percent of the maximum fairing height. A model with only a wheel was used as a control. Parameters maintained constant between different fairing designs included the models' chord length, height,

width, front profile, top profile, wheel size, rate of curvature, and the fairings' design upstream of the wheel's axel. Further control variables in the manufacturing and testing of the models are described below. In the wind tunnel, all the above fairing designs and a control wheel were tested. In the water channel, only the control wheel, 0%H fairing and a 30%H fairing were tested to cover both ends of the fairing height spectrum.

Wind Tunnel

Models were 3d printed out of polylactic acid (PLA) with a Prusa i3 Mk3 (Prusa Research, Czech Republic) at a chord length of 9cm. A model mount was 3d printed, inserted into the models, and fastened using an adhesive. This mounting system was controlled between different models and kept as a constant, as to not skew data between models. Models were finished through a process of repeatedly spray painting and wet sanding. The models' spray paint was sanded down to until the 3d print showed through, ensuring that the original model and shape were not altered, rather only the spray paint was sanded. This process was repeated three times per model until smooth (Figure 3). The fairings were tested at the High School's JetStream 500 wind tunnel (Interactive Instruments, NY, USA)(Figure 4). The fairings were tested on the same day in an indoor temperature regulated facility. Data was taken using the JetStream500's force transducer. The force transducer was calibrated before testing and U_{∞} was verified using a pitot tube, which measures airflow velocity.

For all models, the same wind tunnel settings were used: α was kept constant at 0° and U_{∞} was altered between 0m/s and 27m/s in increments of roughly 2m/s, resulting in a maximum Re of 1.5×10^5 . Measurements were taken on the drag force measured in lb.



Figure 3. Fairings tested in the wind tunnel. From left to right: control wheel, 0%H, 15%H, 30%H.



Figure 4. Jet Stream 500 wind tunnel and testing setup.

Water Channel

The 0%H fairing, 30%H fairing, and control wheel were 3d printed out of PLA with a Prusa Mini (Prusa Research, Czech Republic) at a $c = 17.5$ cm. A $\frac{1}{4}$ in (0.64 cm) threaded rod was mounted in the fairing models, and a National Advisory Committee of Aeronautics (NACA) 0012 airfoil was used to cover the threaded rod to

minimize the drag of the mounting system (Figure 5). The smallest chord possible was used for the NACA 0012 while still housing the threaded rod. Each model was printed in two pieces, with the seam traversing across the NACA 0012 airfoil in the model mount, ensuring the fairings were printed in one piece. The two prints were adhered with epoxy to one another. Models were finished through the same process as described in the wind tunnel section. The spray painting and wet sanding process was repeated 4 times per model until smooth.

Models were tested at the University of Southern California's Fluid Structure and Interactions Lab (Figure 6). Models were mounted upside down onto a traverse used for alignment. Vertically and laterally, models were mounted in the center of the water channel (cross-section 0.9mx0.4m) to avoid wall effects. Data was taken at $U_{\infty}=0.6\text{m/s}$, the maximum speed achievable in order to most closely match the Re . α was kept constant at 0° for all tests, through the 3d printed model mount and leveling of the traverse. Rotation of the model was set to 0° using the force transducer to sense any rotation and using a range finder. A laser sheet was produced by a 5W continuous wave laser with a 10° diverging lens. The laser sheet was aligned with the center of the top of the models where the differences in the height of the trailing edge between fairings were most notable (Figure 6). $20\mu\text{m}$ polyamide particles (LaVision, Germany) were mixed in the water for particle imaging velocimetry (PIV). Imaging data was collected with a Phantom VEO-E 310L camera (1280x800 pixel, 12bit, Vision Research, USA) at 300fps in order to get a 10 pixel displacement of freestream particles per image.



Figure 5. Fairings tested in the water channel. From left to right: 0%H, 30%H, control wheel.

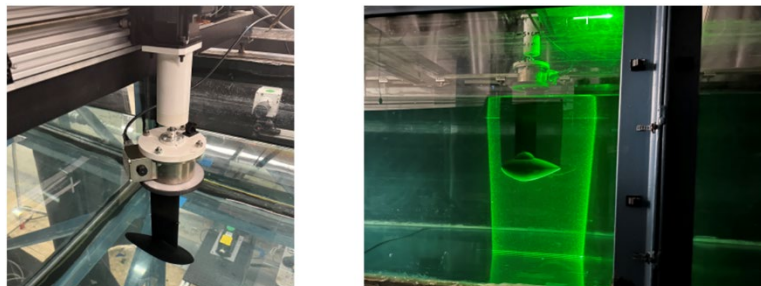


Figure 6. Experimental setup at the University of Southern California's Fluid Structure Interactions Lab. Shown is a fairing suspended upside down and its mount inside the water channel (left). The channel is illuminated from below by a laser sheet for collection of particle image velocimetry data (right).

Data Analysis

Quantitative wind tunnel data was collected on drag force (lb) and plotted graphically without further post processing. Water channel data was analysed using MATLAB R2022a and PIVlab (a graphical user interface to

capture, visualize, and analyze PIV data, The Mathworks, Inc., MA, USA). Images were analyzed with a multi-pass algorithm to produce vector matrices. Interrogation windows were set to 64×64 , 32×32 , and 16×16 pixels. Time averaged velocity, vorticity (a measure of rotation at a point), and streamline plots were then created. Streamlines were created using a streamline rake of 40 lines plotted based on a time averaged vector field, with velocity and vorticity displayed on a color scale.

Results

Wind Tunnel

Figure 7 depicts the drag force data of the tested fairings and control wheel. As shown in Figure 7a, all fairing models had a significantly smaller F_d than the control wheel. While differences in performance between the models was minimal at lower Re , this was accentuated at higher Re . Amongst the tested fairings, the 0%H fairing consistently had the greatest F_d , especially at higher Re (Figure 7b). The 15%H and 30%H models performed similarly, with the 30%H model having a lower F_d at the highest Re tested.

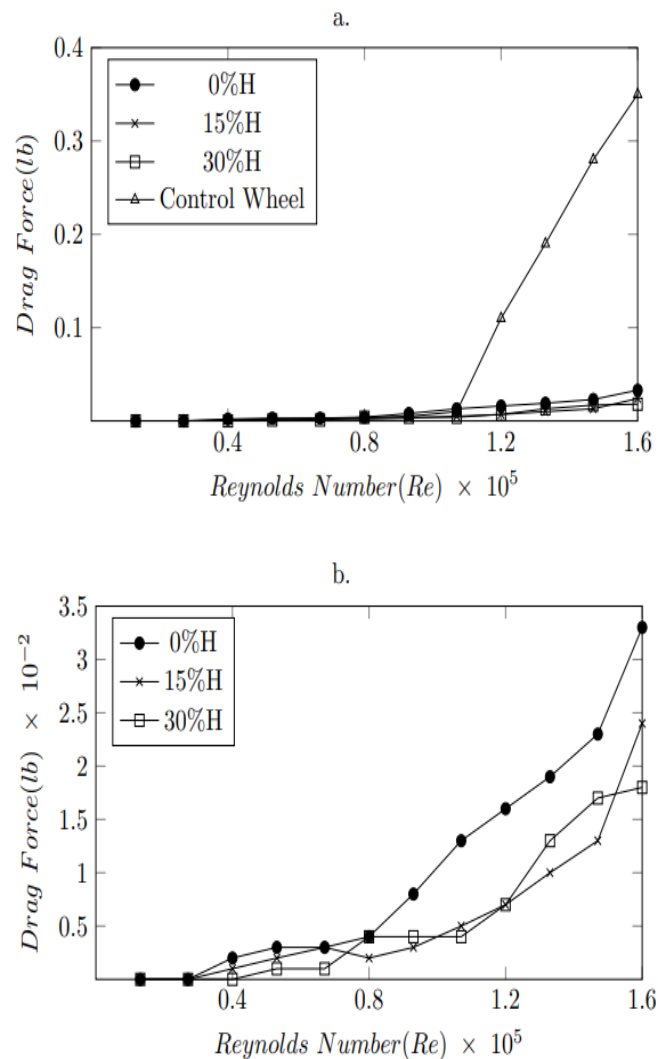


Figure 7. Drag force in the wind tunnel. a) Drag force at different Reynolds numbers for tested fairings and control wheel; $\alpha=0^\circ$ b) Shown is a close up of the fairing data shown in figure 7a.

Water Channel

Figure 8 depicts the horizontal velocity u of the models tested, mounted upside down as depicted in Figure 6, with flow moving from left to right. For all the models we can see the free stream velocity $U_\infty = 0.6\text{m/s}$. For the 0%H, in the velocity deficit trailing the fairing, u was reduced to $u \approx 0.4\text{m/s}$. While the 30%H demonstrated a small stagnant flow region directly behind the trailing edge, the overall area of the velocity deficit was smaller than that of the 0%H. The control wheel exhibited the largest wake in both size and magnitude, with the largest velocity deficit area and with most of the wake having $u \approx 0.12\text{m/s}$ (velocity deficit area: control > 0%H > 30%H).

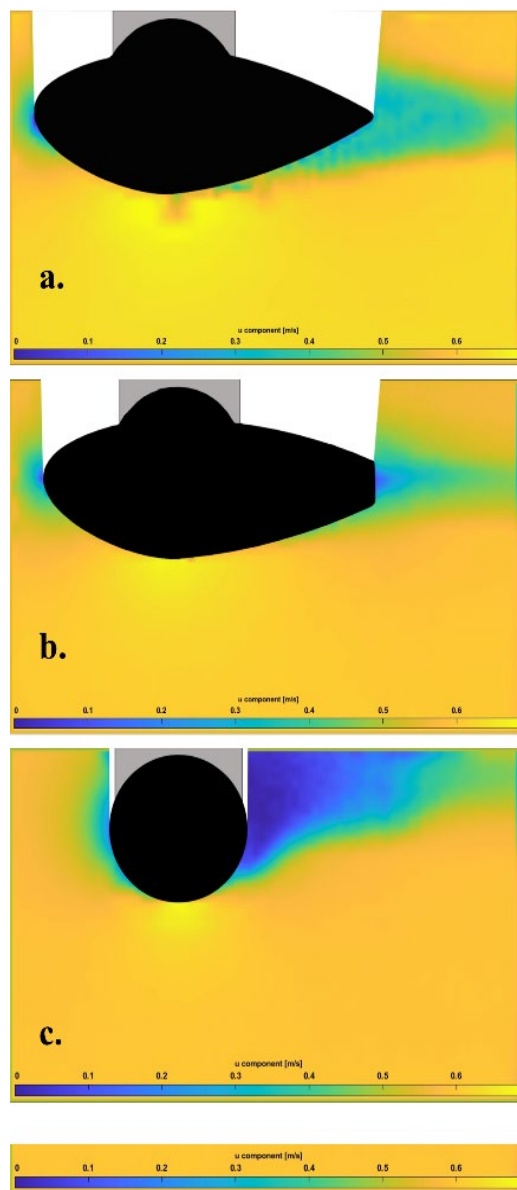


Figure 8. u velocity of the 0%H (a), 30%H (b), and control wheel (c) depicted on a color scale. Also shown are the models (black), the mount (grey), and non-illuminated shadow of the fairing (white).

Figure 9 depicts the vorticities and streamlines for the models. For the models, boundary layer separation occurred near point 1. At point 2 of the 0%H fairing, the vorticity $\approx 35/s$. Despite the fairings having similar streamlines, due to the steeper curvature on the 0%H fairing, greater vorticity was noted at point 2 because the boundary layer was larger. At point 2 in the 30%H fairing, the vorticity $\approx 20/s$.

While the 30%H fairing had an intense local vorticity region just downstream of the trailing edge, the area of flow impacted by vorticities was less than for the 0%H fairing. In the wake further downstream of the fairing (point 3), the 0%H fairing (vorticity ≈ 20 -25/s) exhibited a greater vorticity than the 30%H fairing (vorticity ≈ 10 -15/s). The control wheel had vorticities occurring at $\approx 50/s$ and had the greatest area impacted by vorticities (area of vorticity: control > 0%H > 30%H).

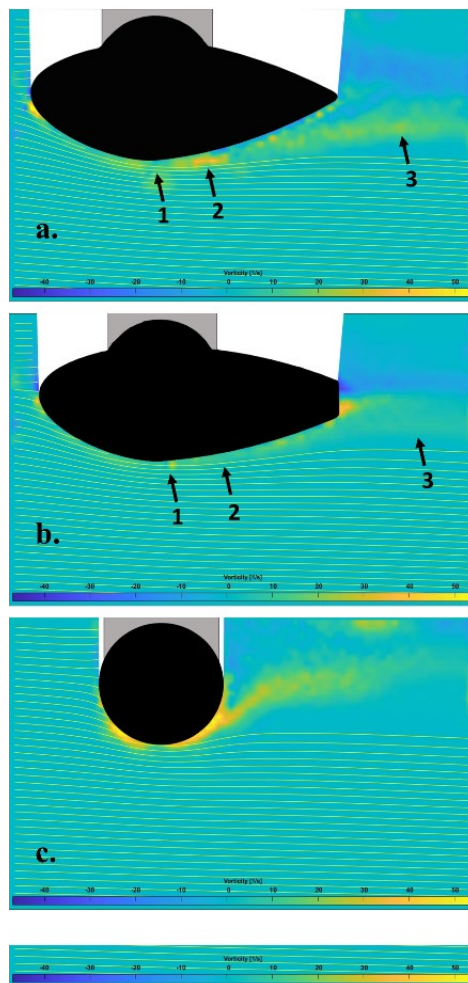


Figure 9. Vorticities of the 0%H (a), 30%H (b), and control wheel (c) depicted on a color scale. Superimposed are streamlines of the fluid flow. Also shown are the fairings (black), the mount (grey), and non-illuminated shadow of the fairing (white).

Discussion

The wind tunnel results confirmed that housing landing gear inside a fairing reduces the drag force. Results of the water channel testing provided complementary information. Here housing landing gear inside a fairing minimized the velocity deficit and vorticity of the trailing edge. The 0%H fairing created a velocity deficit and vorticity in its wake in the water channel that was broader in area than that seen with the 30%H fairing (Figure 8), consistent with the larger drag coefficient for the 0%H fairing as assessed in the wind tunnel (Figure 7). Thus, while the wake of a 30%H fairing may show small local maxima of greater velocity deficit and vorticity compared to a 0%H fairing, overall the area of impact on reducing velocity and increasing vorticity is less. These results are consistent with those of the wind tunnel in which for fairings of the same length, a less pointed trailing edge delivers an improved drag performance.

My results extend the early work by Herrnstein and Biermann who in their work examined the force of drag in pounds acting upon 8 different types of fairings at 80 and 100 miles per hour via the use of a wind tunnel. Their designs focused on fairings with a pointed 0%H trailing edge, while examining the effects of parameters related to fairing width (Herrnstein and Bierman, 1934). The current study's results now suggest also the importance of the design of the trailing edge in minimizing drag.

Limitations

The presence of both velocity deficits and vorticity at the trailing edge can impact the drag force experienced by a fairing. However, the relationship is not straightforward and depends on numerous factors, including the aircraft speed and operating conditions (takeoff, cruise, landing) (Shelton, 2023). While data from multiple experiments was sourced to verify the results, due to limitations of available wind speeds in the wind tunnel and flow speeds in the water channel, data was taken at a lower Re (directly correlated to flight speed) than typical general aviation aircraft fly. Wind tunnel tests were done at $Re = 1.5 \times 10^5$ and the water channel tests were done at $Re = 1.1 \times 10^5$, while typical applications for fairings, ultralight aircraft and small general aviation aircraft, fly between 1.0×10^6 Re and 1.0×10^7 Re (Lissaman, 1983). The Re used in the current experiments was set to the maximum possible Re for the available experimental set up. We did not test the effects of length of the leading edge, width of the fairing, or other design parameters. Furthermore, we did not test effects of changes in the pitch or yaw angle, air temperature or presence of fuselage or propeller slip stream on drag coefficients. Future work will need to address these parameters.

Conclusion

Integrating wheel fairings into landing gear increases the wake velocity, while decreasing the drag force and vorticity. Optimization of the design of the trailing edge can further improve efficiency of a fairing by increasing the height of the trailing edge from a 0% height (pointed) to a broader profile.

Acknowledgments

I would like to thank Professor Geoffrey Spedding, Ph.D. at the University of Southern California (USC) for his advice and access to USC's Fluid Structure and Interactions Lab. I also want to thank Gerard Lynch at the high school for help in setting up the wind tunnel. In particular, I want to thank Chase Klewicki, B.S., M.S. at USC for his guidance in the experimental setup of the water channel.

References

Ablog, D., Fuget, M., Ko, S., Tsujita, K. (2014). "Optimization of Landing Gear Fairings", Final report to the American Institute of Aeronautics and Astronautics, pp. 1-17.

Götten, F., Finger, D.F, Havermann M, Braun C, Gomez F, Bil C. (2018). "On the Flight Performance Impact of Landing Gear Drag Reduction Methods for Unmanned Air Vehicles", Deutsche Gesellschaft für Luft- und Raumfahrt - Lilienthal-Oberth e.V.. (conference paper). <https://doi.org/10.25967/480058>. urn:nbn:de:101:1-2018121411573397502495

Herrnstein, Jr., W., Biermann, D. (1934). "The Drag of Airplane Wheels, Wheel Fairings, and Landing Gears-I", Report of National Advisory Committee for Aeronautics, Report 485, pp. 193-222.

Lissaman, P.B.S. (1983). "Low-Reynolds-Number Airfoils", Annual Review of Fluid Mechanics, Vol. 15 pp. 223-39.

Shelton, N. "Induced Drag: How It Works" (2023). <https://www.boldmethod.com/learn-to-fly/aerodynamics/how-induced-drag-works-lift/>, Boldmethod, Boulder, Co.

The pilot's manual editorial team (2016). "The Pilot's Manual: Ground School: Pass the FAA Knowledge Exam and operate as a private or commercial pilot", Aviation Supplies Academics, Inc., 6th edition, Newcastle, MA.

Wojnar, R. (1967). "The Effects Of Landing Gear Configuration On The Drag Of Homebuilt Aircraft", Experimental Aircraft Association: Sport Aviation, pp. 7-10.